Molecular Therapy
Nucleic Acids
Original Article

Axl-Targeted Delivery of the Oncosuppressor miR-137 in Non-small-Cell Lung Cancer

Silvia Nuzzo,[1,8] Silvia Catuogno,[2,8] Maria Capuozzo,[2] Alfonso Fiorelli,[3] Piotr Swiderski,[4] Serena Boccella,[5] Filomena de Nigris,[6,7] and Carla Lucia Esposito[2]

[1]IRCCS SDN, Naples, Italy; [2]Istituto di Endocrinologia ed Oncologia Sperimentale, Consiglio Nazionale delle Ricerche (CNR), Naples, Italy; [3]Thoracic Surgery Unit, University of Campania "Luigi Vanvitelli," Naples, Italy; [4]DNA/RNA Synthesis Laboratory, Beckman Research Institute of City the of Hope, Duarte, CA, USA; [5]Department of Experimental Medicine, University of Campania "Luigi Vanvitelli," Naples, Italy; [6]Department of Precision Medicine, University of Campania "Luigi Vanvitelli," Naples, Italy; [7]Sbarro Institute for Cancer Research and Molecular Medicine, Center for Biotechnology, College of Science and Technology, Temple University, Philadelphia, PA, USA

Non-small-cell lung cancer (NSCLC) accounts for 85%–90% of all cases of lung cancer that is the most deadly type of cancer. Despite advances in chemotherapy and radiotherapy, severe side effects and frequent drug resistance limit the success of the treatments, and the identification of new therapeutic options still represents a crucial challenge. Here, we provide the evidence for the therapeutic potential of an aptamer-microRNA (miR) complex (AmiC) composed by an aptamer (GL21.T), able to bind and antagonize the oncogenic receptor Axl, and the miR-137, downregulated in lung cancer and involved in cell survival and proliferation. We found that, when applied to Axl-expressing NSCLC cancer cells, the complex is effectively internalized, increasing miR cellular levels and downregulating miR targets. Most importantly, the complex combines the inhibitory function of the GL21.T aptamer and miR-137, leading to a negative impact on NSCLC migration and growth. The described AmiC thus represents a promising tool for the development of new therapeutic approaches for NSCLC.

INTRODUCTION

Lung cancer is the leading cause of cancer-related death in the world, with non-small-cell lung cancer (NSCLC) representing approximately 80% of all lung cancer.[1,2] Median survival time of patients with NSCLC after diagnosis is generally less than 1 year. In addition, NSCLC cells often retain the ability to evade drug-induced death signals, and relapses are frequent.[3] Thus, the identification of new therapeutic options is a crucial challenge in oncology.

MicroRNAs (miRs) are short non-coding RNAs that regulate gene expression by causing either inhibition of mRNA translation into proteins and/or mRNA degradation.[4] They are emerging as promising therapeutic tools for cancer therapy.[5] Among other miRs, miR-137 has been found to be downregulated and to act as a tumor suppressor in several cancers, including NSCLC. It has been demonstrated that a high miR-137 expression correlates with a higher NSCLC patient survival[6] and that it regulates cell proliferation and tumor growth.[7–9]

Despite their therapeutic potential, miRs' specific delivery to tumor cells still represents an essential step for their clinical development. In recent years, great hope for the selective delivery of miRs has emerged from the use of nucleic acid aptamers as targeting agents. They are high-affinity ligands and potential antagonists of disease-associated proteins and have many advantages as therapeutic agents and effective delivery carriers for the specific and safe diffusion of secondary reagents into tumor cells.[10] Several studies have demonstrated the broad applicability both *in vitro* and *in vivo* of aptamer-mediated delivery of therapeutic small interfering RNAs (siRNAs) and miRs.[11–18] In previous studies, we reported the generation of 2′-fluoropyrimidine (2′F-Py) nuclease-resistant RNA aptamer, named GL21.T, binding and antagonizing the oncogenic receptor tyrosine kinase Axl.[19] We showed that GL21.T can be used for the selective delivery to Axl^+ cells of therapeutic miR-based molecules.[16,17] By applying a stick-based approach, this aptamer was recently linked to miR-137, generating a complex (named GL21.T-137) to target glioblastoma cancer stem-like cells.[18]

Given the promising role of miR-137 in NSCLC, in this paper we analyzed the functional effect of GL21.T-137 aptamer-miR complex (AmiC) on lung cells.

Our results show that GL21.T-137 treatment leads to inhibiting NSCLC migration and survival by combining both the inhibitory function of GL21.T aptamer on Axl receptor and the reduction of miR-137 targets. In addition, GL21.T-137 complex demonstrated to effectively reduce tumor growth *in vivo* in NSCLC mouse xenografts.

The described complex has a broad applicability to cancer treatment and represents a potential tool for NSCLC treatment.

Received 26 March 2019; accepted 4 June 2019;
https://doi.org/10.1016/j.omtn.2019.06.002.

[8]These authors contributed equally to this work.

Correspondence: Carla Lucia Esposito, Istituto di Endocrinologia ed Oncologia Sperimentale, Consiglio Nazionale delle Ricerche (CNR), Via T. de Amicis, 80131 Naples, Italy.
E-mail: c.esposito@ieos.cnr.it

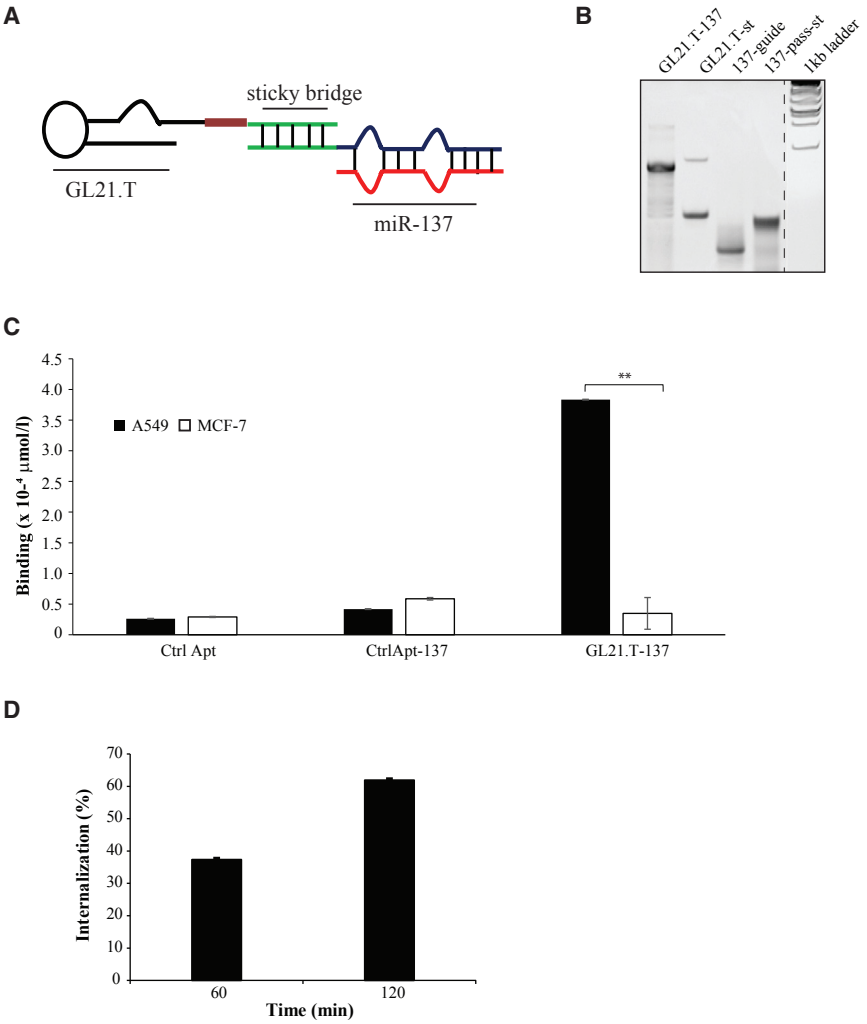

Figure 1. GL21.T-137 Preparation, Binding, and Internalization

(A) Scheme of GL21.T-137 AmiC based on stick-end annealing. (B) The annealing efficacy was confirmed by loading each component or annealed conjugate on a 12% non-denaturing polyacrylamide gel followed by staining with ethidium bromide. GL21.T-st, GL21.T sticky; 137-pass-st, miR-137 passenger strand sticky; 137-guide, miR-137 guide strand. (C) Binding of 200 nmol/L GL21.T-137, control aptamer (Ctrl Apt), or control complex (CtrlApt-137) on A549 (Axl^+) versus MCF-7 (Axl^-) cells measured by qRT-PCR after 30 min of incubation. Statistics were calculated using Student's t test, $^{**}p < 0.01$. (D) Internalization of 200 nmol/L GL21.T-137 was monitored by qRT-PCR (see Materials and Methods for details). The percentage of internalization is expressed as the amount of internalized RNA relative to total bound RNA.

RESULTS

GL21.T-137 Conjugate Binding and Internalization in NSCLC

We have recently designed a multifunctional complex (GL21.T-137) in which the GL21.T aptamer, an Axl receptor antagonist, is used as a delivery carrier for miR-137.[18] For the complex generation, we used a stick-based strategy (Figure 1A). As we previously reported,[16,19] we derived the miR mimetic portion from the distal stem of the human miR-137 precursor using 29 bases of the 5′ strand and 28 of the 3′ strand, in order to produce an internal partial complementarity and a more effective Dicer substrate.[20] The annealing efficiency was monitored by the presence of a shifted band of migration on a non-denaturing gel (Figure 1B). Considering that it has been shown that miR-137 functions as an oncosuppressor in NSCLC and that high miR-137 levels correlate with a higher survival rate,[6–9] we analyzed GL21.T-137 complex on NSCLC cells.

As a first attempt, we analyzed whether in the context of the AmiC the aptamer preserves a good binding ability on A549 (Axl^+) NSCLC cells. We used as negative control MCF-7 (Axl-) cells, on which we have already found no detectable binding of the GL21.T aptamer.[16,17,21] As shown in Figure 1C, the GL21.T-137 complex preferentially binds target A549 (Axl^+) cells compared to the MCF-7 (Axl^-) cells. No discrimination was detected by treating either with a control aptamer (CtrlApt) or with a control complex containing the CtrlApt linked to miR-137 (CtrlApt-137), supporting that the GL21.T-137 complex specifically targets Axl-expressing cells. This result is in good agreement with data obtained for the GL21.T aptamer[21] or GL21.T complexes containing other therapeutic RNA cargoes.[6,17]

We have previously reported that the GL21.T aptamer alone or conjugated to Let-7g miR rapidly internalizes into A549 (Axl^+), getting about 60% of internalization at 2 h of incubation.[16] We thus checked whether the presence of miR-137 could alter this function. To this end, high-salt washes were used to remove cell-surface-bound molecules and recover the internalized fraction.[22] Total bound or internalized fractions were measured by qRT-PCR. In accordance with previous data, we found that GL21.T-137 preserves GL21.T internalization property on A549 cells and reaches about 62% of internalization after 2 h (Figure 1D). The same result was obtained by using proteinase K (PK) treatment to remove cell-surface molecules (Figure S1). These data confirm that GL21.T-137 preserves aptamer binding ability and internalization in Axl^+ NSCLC cells.

GL21.T-Mediated Functional Delivery of miR-137 in NSCLC

As a next step, we confirmed that GL21.T-137 increases intracellular miR-137 levels at a comparable extent of a commercial miR-137 mimic upon transfection (Figure S2), thus preserving miR moiety function as well. Thus, we analyzed whether the treatment of A549 Axl-expressing cells may effectively increase the corresponding

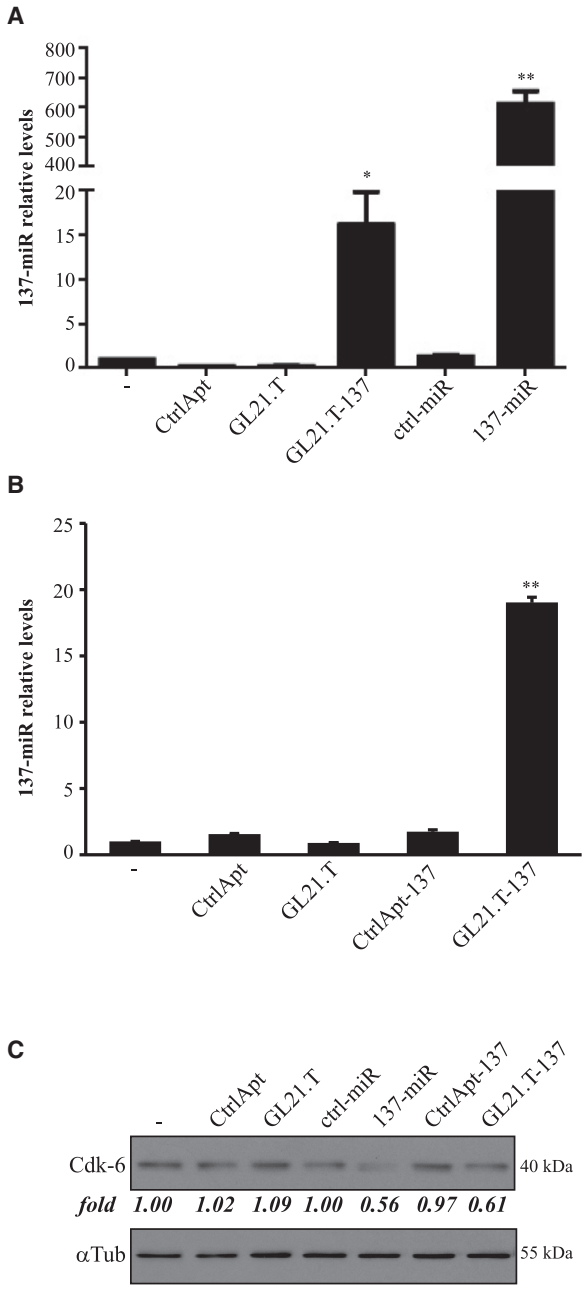

Figure 2. GL21.T-Mediated Delivery of miR-137

(A) A549 cells (Axl$^+$) were transfected with 100 nmol/L of miR-137 or control miR (ctrl-miR) or treated with 400 nmol/L GL21.T, control aptamer (CtrlApt) or GL21.T-137. After 24 h, miR-137 levels were measured by qRT-PCR. (B) Levels of miR-137 detected in A549 cells (Axl$^+$) treated with 400nmol/L indicated aptamers or conjugates. (A and B) Error bars depict mean ± SD. Statistics were calculated using Student's t test (versus untreated), **$p < 0.05$, **$p < 0.01$. (C) The levels of Cdk6 were analyzed by immunoblotting following 48 h. Anti-α-tubulin (αTub) antibodies were used as a loading control. Values below the blots indicate quantization relative to untreated ("–," for treatment) or ctrl-miR (for transfection) normalized on the loading control signals. Molecular weights of indicated proteins are reported.

endogenous miR. In our previous report, we showed that 400 nmol/L treatment effectively assures a functional GL21.T-mediated miR delivery.[16] Therefore, A549 cells were treated with 400 nmol/L of GL21.T-137, and the levels of miR-137 were determined by qRT-PCR. As shown, the AmiC treatment results in a significant increase of miR levels as compared with GL21.T or control aptamer (Figure 2A), even though with several folds of difference in respect to miR-137 mimic transfection. Notably, the levels of miR-137 are not affected when cells are treated with a control complex (Figure 2B), thus confirming that miR-137 upregulation is dependent on the presence of the GL21.T aptamer in the complex rather than on non-specific molecular interactions. Then, we analyzed the levels of Cdk6, a validated miR-137 target.[8] As shown in Figure 2C, GL21.T-137 treatment reduces Cdk6 of about 40% at 48 h compared to the control aptamer or the control complex. Of note, the extent of inhibition was comparable to the data obtained upon miR transfection (44% reduction compared to control miR) despite the significantly higher levels of miR-137 measured upon transfection (Figure 2A). This data suggests that the higher miR levels are not required to have an effect on the target but are likely related to off-target effects.

Together, these experiments show that the AmiC effectively delivers functional miR-137 in NSCLC cells.

GL21.T-137-Mediated Inhibition of NSCLC Cell Motility and Viability

The GL21.T-137 AmiC combines two functional moieties, consisting of the GL21.T aptamer that is able to neutralize the Axl receptor activity inhibiting cell migration[21] and miR-137, which has been described to be implicated in NSCLC survival and proliferation.[8] Thus, we next analyzed the combined functional effects of the AmiC on NSCLC cells.

We have previously reported that the GL21.T aptamer is able to inhibit ligand-dependent Axl tyrosine kinase activity (at 200 nmol/L concentration).[21] We first investigated the ability of the AmiC to preserve this function. As shown in Figure 3A, inhibition of Gas6-dependent Axl activation is comparable between the GL21.T aptamer and the GL21.T-137 complex, confirming that the conjugation of the miR to the aptamer does not abrogate aptamer function. Consequently, the GL21.T-137 complex inhibits A549 (Axl$^+$) cell migration at a level comparable to that of the GL21.T aptamer, reaching about 80% of inhibition (versus 75% for GL21.T). This effect mainly derives from the aptamer moiety, since the miR-137 transfection does not efficiently alter cell migration (Figure 3B). No reduction was detected by treating with the control aptamer or the control complex.

Then, we analyzed the complex functional effects dependent on the presence of miR-137. We found that the complex reduces A549 cell viability of approximately 30% following 72 h. On the contrary, no significant effect was detected by the GL21.T aptamer alone or in the presence of the CtrlApt or the CtrlApt-137 complex (Figure 4A). Further, in accordance with previous findings on miR-137 function in NSCLC,[8] the GL21.T-137 treatment results in the downregulation of

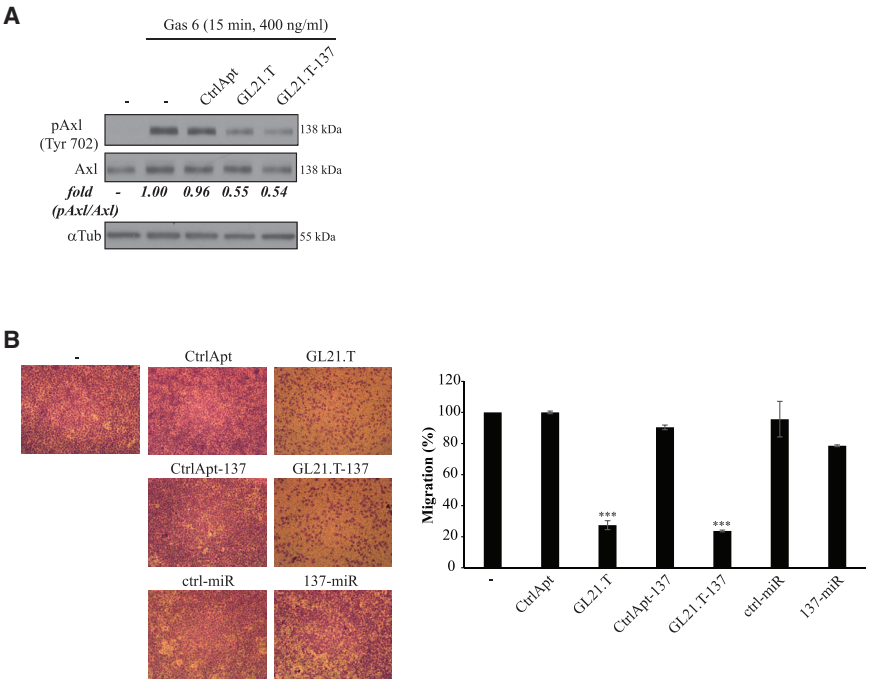

Figure 3. GL21.T-137 Effect on Axl Activity and Migration

(A) Serum-starved A549 (Axl$^+$) cells left untreated or treated for 3 h with 200 nmol/L of control aptamer, GL21.T, or GL21.T-137 were stimulated with Gas6 in the presence of each RNA. Cell lysates were immunoblotted with anti-phospho-Axl (pAxl(Tyr702)), anti-Axl, and anti-α-tubulin antibodies. Quantization of the ratio of pAxl/Axl relative to untreated are indicated below the blots. Molecular weights of indicated proteins are reported. (B) A549 (Axl$^+$) cells were transfected with 100 nmol/L ctrl-miR or miR-137 or treated with 400 nmol/L of GL21.T, Ctrl Apt, CtrlApt-137, or GL21.T-137 and cell migration was analyzed by transwell migration assay. Left panel: migrated cells were stained with crystal violet and photographed. Right panel: migrated cells were quantified and expressed as percent of migrated cells with respect to untreated cells. Error bars depict mean ± SD. Statistics were calculated using Student's t test, ***$p < 0.001$ (versus untreated).

the cyclin D1 and of the phosphorylated Rb, downstream miR-137 targets involved in cell proliferation[8] (Figure 4B). We also analyzed the conjugate action in combination with the chemotherapeutic Paclitaxel and the epidermal growth factor receptor (EGFR) tyrosine kinase inhibitor Erlotinib that are currently in clinical use as anti-cancer therapeutics. In our experimental conditions, A549 resulted resistant to Erlotinib, whereas a significant reduction of cell viability was found with Paclitaxel or GL21.T-137 treatment. No improvement of sensitivity was observed upon combined regimes of either Erlotinib or Paclitaxel and the complex treatment or miR-137 transfection (Figure S3).

Collectively, these results indicate that the AmiC combines GL21.T and miR-137 functions, inducing an impaired cell motility (mediated by the aptamer moiety) and viability (mediated by the miR moiety).

GL21.T-137-Mediated Activity in Patient-Derived NSCLC Cells and *In Vivo*

In order to extend the AmiC functional characterization, we determined the effects of the GL21.T-137 in Axl$^+$ primary cells (NSCLC #17 and #18) obtained from surgical specimens from lung cancer patients (Figure S4). Cells were treated with 400 nmol/L GL21.T aptamer or GL21.T-137 complex and the effects on cell viability and migration were analyzed. As shown in Figure 5, the aptamer and the complex treatments efficiently hamper cell migration (Figures 5A and 5B), reaching about 40% of inhibition in both cell lines as compared to a control aptamer or a control complex. Further, the GL21.T-137 complex significantly reduces cell viability in both cell lines (Figures 5C and 5D), confirming GL21.T-137 functional activity on NSCLC.

Next, to assess the effect of the GL21.T complex on tumor growth *in vivo*, A549 tumor-bearing mice were treated with the GL21.T or GL21.T-137 AmiC (1,600 pmol/injection) by intraperitoneal administration. As shown (Figure 5E), after 1 week of treatment, the GL21.T treatment induces a significant reduction of tumor growth that is further inhibited by the GL21.T-137 complex. In addition, histopathological analyses revealed that, as compared to the control group, the GL21.T-137-treated tumors showed a reduction of the cellularity (Figure 5F).

DISCUSSION

The use of aptamers for targeted delivery of interfering RNA molecules (siRNAs, miRs, and miR inhibitors) is emerging as a promising therapeutic strategy in cancer, aimed to enhance the therapeutic efficacy, reducing the occurrence of unwanted off-target effects on healthy tissues.[23] In a previous study, we developed the GL21.T aptamer, demonstrating its ability to bind and inhibit Axl receptor activity, reducing cell migration and tumor growth.[21] Recently, we have described that an AmiC (named GL21.T-137) containing the GL21.T aptamer and miR-137 is able to effectively reach and inhibit glioma stem cells phenotype in a receptor-dependent manner. The AmiC was shown to remain stable up to 8 h in 80% serum.[18]

Here, we address the therapeutic applicability of the GL21.T-137 complex to NSCLC, demonstrating its ability to selectively bind to Axl-expressing NSCLC cells (Figure 1) and produces within target cells a functional miR-137 (Figure 2), thus leading to impairment of cell migration and viability *in vitro* and altering of tumor growth *in vivo* (Figures 3, 4, and 5). Notably, compared to miR mimic transfection, the treatment permits the same extent of inhibition with a more physiological level of miR, thus greatly reducing the potential occurrence of off-target effects.

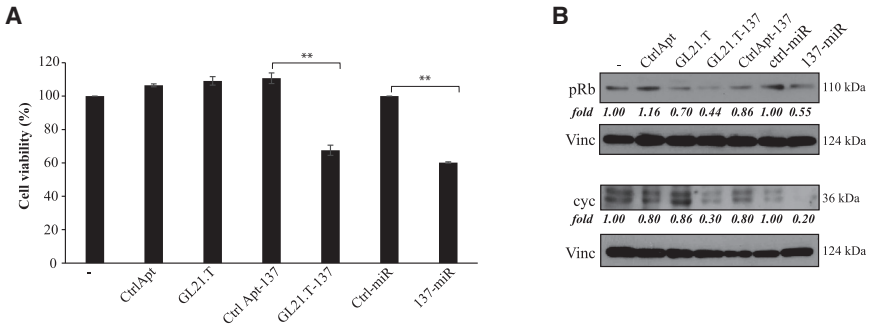

Figure 4. GL21.T-137 Effect on Cell Growth

(A) A549 (Axl$^+$) cells were transfected with 100 nmol/L miR-137 or ctrl-miR or treated with 400 nmol/L Ctrl Apt, CtrlApt-137, GL21.T-137, or GL21.T. After 72 h, cell viability was measured by MTT assay and expressed as percentage of viable cells relative to untreated ("−," for treatment) or ctrl-miR (for transfection). Error bars depict mean ± SD. Statistics were calculated using Student's t test, **$p < 0.01$. (B) Cell lysates from A549 (Axl$^+$) cells treated with GL21.T-137, CtrlApt-137, GL21.T, or CtrlApt or transfected with 100 nmol/L of miR-137 or control miR (ctrl-miR) were immunoblotted with anti-cycD1, anti-phospho-Rb (pRb), and anti-vinculin (Vinc) antibodies. Values below the blots indicate normalized quantization of signal levels relative to untreated ("−," for treatment) or ctrl-miR (for transfection). Molecular weights of indicated proteins are reported.

Our data reveal the therapeutic potential of the GL21.T-137 in NSCLC, showing its ability to act as a multifunctional molecule affecting both cell survival and migration through the combination of the Axl-signaling inhibition, mediated by the GL21.T aptamer, and the anti-tumor growth properties of the miR-137. The used AmiC thus gives the possibility to have different functional effects in a unique molecule, well-fitting with the increased interest in the use of combination therapies in cancer.

The two moieties of the GL21.T-137 complex have attractive potential for NSCLC therapeutic targeting. The GL21.T aptamer targets the receptor tyrosine kinase Axl, whose expression has been correlated to malignant progression and metastasis in lung cancer.[24–26] Further, it has been demonstrated to be a fundamental role of Axl in regulating lung cancer cell invasion and metastasis[27,28] and its involvement in the resistance to tyrosine kinase inhibitors.[29,30] These studies highlight the therapeutic potential of the Axl-targeting therapies for NSCLC. On the other hand, it has been demonstrated that miR-137 acts as a tumor suppressor in NSCLC, being downregulated in NSCLC tissue samples and inhibiting cell proliferation of NSCLC cells when increased.[7,8]

Our results provide a first description of the functional effects of the combination of Axl inhibition and miR-137 increase in NSCLC. Importantly, the ability of the AmiC to affect patient-derived cells and interfere with tumor growth in xenograft mouse models revealed favorable prospects for a further *in vivo* development of the molecule. In addition, the use of chemically modified nucleotides enhances the safety of the AmiC, minimizing the potential of non-specific immunostimulatory effects[16] and enhancing serum stability.[18]

In conclusion, our data demonstrate a broad applicability of the miR-137 AmiC in cancer therapy, indicating that it has the potential to target Axl-expressing cancer cells interfering with multiple processes and may be developed for NSCLC treatment.

MATERIALS AND METHODS

Cell Culture and Transfection

Cell lines were purchased from the ATCC (LG Standards, Milan, Italy). Human NSCLC A549 (Axl$^+$) were grown in RPMI medium supplemented with 10% fetal bovine serum (FBS); human breast MCF-7 (Axl$^-$) cells were grown in DMEM supplemented with 10% FBS.

To prepare primary cell cultures, human lung biopsies (samples from Azienda Ospedaliera Universitaria Primo Policlinico, Naples, Italy) were cut mechanically. Isolated cells were grown in DMEM/nutrient F12-Ham (DMEM-F12) supplemented with 10% FBS. All cell culture reagents were purchased from Sigma (St. Louis, MO, USA).

Transfections were performed using serum-free Opti-MEM and Lipofectamine 2000 reagent (Thermo Fisher Scientific, Waltham, MA, USA). In brief, cells were seeded in 6-well plates (1.4×10^5 cells/well) or in 96-well plates (3×10^3 cells/well), and transfections were performed in the presence of 3 μL or 0.2 μL Lipofectamine 2000, respectively. Cells were transfected with 100 nmol/L of pre-miR miR precursor miR-137 (miR-137) and negative control #1 (ctrl-miR) (Thermo Fisher Scientific, Waltham, MA, USA).

Aptamer-miR Complexes

GL21.T: 5′-AUGAUCAAUCGCCUCAAUUCGACAGGAGGCUCAC-3′;

Control aptamer (CtrlApt): 5′-GCACGCAAAUAGCGACUUCAGACGACUCUUCAGU-3′;

GL21.T stick: 5′-AUGAUCAAUCGCCUCAAUUCGACAGGAGGCUCACXXXXGUACAUUCUAGAUAGCC-3′;

Control aptamer stick: 5′-GCACGCAAAUAGCGACUUCAGACGACUCUUCAGUXXXXGUACAUUCUAGAUAGCC-3′;

miR-137 passenger stick: 5′-GGUGACGGGUAUUCUUGGGUGGAUAAUAGGCUAUCUAGAAUGUAC-3′;

miR-137 guide (3p): 5′-UGUUAUUGCUUAAGAAUACGCGUAGUCUU-3′.

RNA sequences were synthesized by DNA/RNA Synthesis Laboratory at the Beckman Research Institute of City of the Hope (Duarte, CA, USA) or Tebu-bio srl (Magenta, Milan, Italy) and contained 2′F-Py. Stick sequences (underlined) consist of 2′F-Py and 2′-oxygen-methyl

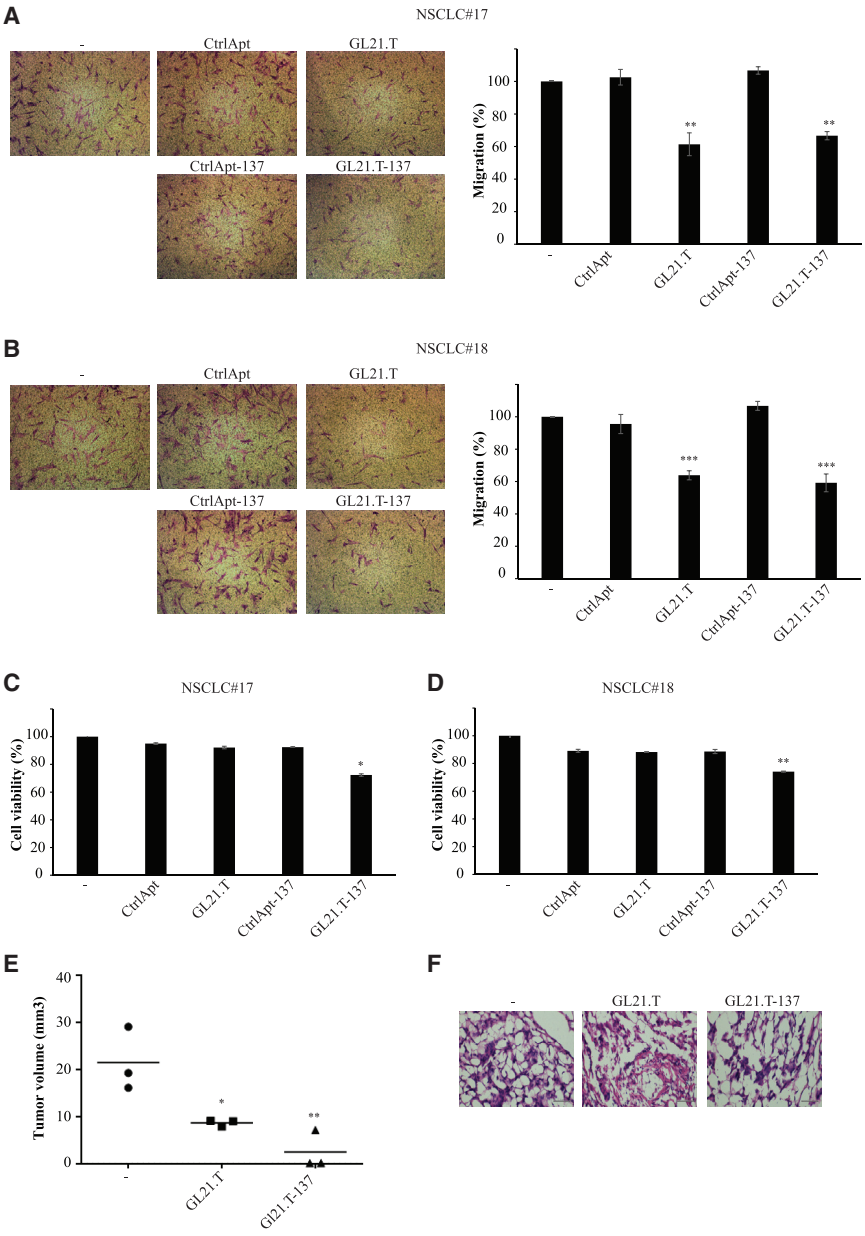

Figure 5. GL21.T-137 Effect on Patient-Derived Cells and *In Vivo*

(A–D) NSCLC patient derived cells (#17 and #18, Axl$^+$) cells were treated with 400 nmol/L of GL21.T, Ctrl Apt, CtrlApt-137, or GL21.T-137. (A and B) Cell migration of NSCLC patient cells #17 (A) or #18 (B) was analyzed by transwell migration assay. Migrated cells were stained with crystal violet and photographed. Left panels: representative micrographs are shown. Right panels: migrated cells were quantified and expressed as percent of migrated cells with respect to untreated cells (–). (C and D) Following 72 h of treatments, cell viability of NSCLC patient cells #17 (C) or #18 (D) was measured by MTT assay and expressed as percentage of viable cells relative to untreated (–). In (A)–(D), error bars depict mean ± SD. Statistics were calculated using Student's t test, $^{**}p < 0.01$; $^{***}p < 0.001$ (versus untreated). (E) Plot representation of tumor volume in A549 mouse xenograft models following 7 days of PBS (–), GL21.T, or GL21.T-137 treatment by intraperitoneal injection. Statistics was performed with GraphPad Prism v.6.0 by ANOVA (n = 3). $^{*}p < 0.05$, $^{**}p < 0.01$. (F) Representative sections of tumors from the PBS, GL21.T, and GL21.T-137 groups stained with H&E. Magnifications, 40×.

purines. The italic X indicates a covalent spacer, a three-carbon linker ((CH2)3). Before each treatment, aptamers were subjected to a short denaturation-renaturation step (5 min 85°C, 3 min on ice, 10 min at 37°C). For complex generation, (1) miR-137 passenger and guide were annealed in buffer (20 mM HEPES [pH 7.5], 150 mM NaCl, 2 mM CaCl2) at 95°C for 10 min, 55°C for 10 min, and then room temperature for 20 min; (2) stick aptamer was refolded (5 min 85°C, 3 min on ice, 10 min at 37°C); (3) equal amounts (ratio 1:1) of stick aptamer and passenger-guide duplex were then annealed by incubating together at 37°C for 30 min. The annealing efficiency was evaluated on a 12% non-denaturing polyacrylamide gel.

Cell Binding and Internalization Assay by qRT-PCR

Cells (2×10^5 cells/well in 6-well plate) were treated with 200 nmol/L of GL21.T-137 at 37°C in the presence of 100 μg/mL polyinosine used as a non-specific competitor (Sigma) as indicated and washed three times with PBS (for binding). For internalization, cells were washed three times with 0.5 M NaCl PBS[22] or treated with 0.5 μg/μL proteinase K (Roche Diagnostics, Indianapolis, IN, USA) for 30 min at 37°C[16,31] to remove cell-surface-bound RNA. RNA was recovered by TRIzol (Life Technologies) containing 0.5 pmol/mL of CL4 aptamer (CL4, 5′-GCCUUAG UAACGUGCUUUGAUGUCGAUUCGACAG GAGGC-3′), used as a reference control. The amount of bound RNAs was determined by performing qRT-PCR, as previously reported[17] by using the following primers: GL21.T (forward), 5′-AGATCATGAT CAATCGCC-3′; GL21.T (reverse), 5′-GTGAGCCTCCTGTCGA-3′; CL4 (forward), 5′-GCCTTAGTAACGTGCTTT-3′; and CL4 (reverse) 5′-GCCTCCTGTCGAATCG-3′. The amounts of RNA was calculated relative to a standard curve of known RNA input and normalized to the CL4 reference control. The percent of internalization was expressed as the amount of internalized aptamer relative to total bound aptamer.

miR Level Analyses by qRT-PCR

To assess miR levels, RNAs were extracted with TRiZol (Thermo Fisher Scientific, Waltham, MA, USA) and 500 ng of total RNA

was reverse transcribed with miScript reverse transcription kit (QIAGEN, Milan, Italy) according to the manufacturer's protocol. Amplification was performed by using the miScript-SYBR green PCR kit and miScript primer assay specific for miR-137-3p (QIAGEN, Milan, Italy). U6 RNA was used as a housekeeping control gene.

Immunoblot Analysis

Total cell lysates were prepared in JS buffer (50 mM HEPES [pH 7.5], 150 mM NaCl, 1% glycerol, 1% Triton X-100, 1.5 mM $MgCl_2$, 5 mM EGTA, 1 mM Na_3VO_4, protease inhibitors) and then boiled in SDS/β-mercaptoethanol sample buffer. Proteins were separated by electrophoresis and then blotted onto polyvinylidene difluoride membranes (Millipore, Billerica, MA, USA) by an electrophoretic transfer. After blocking with 5% dried milk in Tris-buffered saline (TBS) containing 0.1% Tween 20, membranes were incubated at 4°C overnight with the following primary antibodies: cyclin-dependent kinase 6 (Cdk6; Santa Cruz Biotechnology, Stockton, CA, USA); phospho-retinoblastoma (pRb; Cell Signaling Technology, Danvers, MA, USA); cyclin D1 (Cell Signaling Technology, Danvers, MA, USA); phospho-Axl (pAxl; Cell Signaling Technology, Danvers, MA, USA); Axl (R&D Systems, Minneapolis, MN, USA); α-tubulin (Santa Cruz Biotechnology, Stockton, CA, USA); vinculin (Cell Signaling Technology, Danvers, MA, USA). Ligand-dependent Axl receptor activation was performed by using Gas6 from R&D Systems. Cells were serum starved overnight, pre-treated with 200 nmol/L GL21.T, CtrlApt, or GL21.T-137 for 3 h, and then stimulated with 400 ng/mL Gas6 either alone or in presence of each aptamer or complex. Blots were quantified with ImageJ software.

Cell Viability

Cells were seeded in 96-well plates (3×10^3 cells/well) and transfected with miR-137 or ctrl-miR or treated with GL21.T, control aptamer, control complex (CtrlApt-137) or GL21.T-137 (400 nmol/L final concentration) for 72 h. For combined regimes, 1 μmol/L Paclitaxel or 1 μmol/L Erlotinib (Sigma, St. Louis, MO, USA) were used. Cell viability was assessed by CellTiter 96 proliferation assay (Promega, Madison, WI, USA) and expressed as percent of viable treated cells with respect to control untreated cells.

Transwell Migration

Cells were seeded in 6-well plates (1.4×10^5 cells/well) and transfected with miR-137 or ctrl-miR or treated with 400 nmol/L GL21.T, control aptamer, CtrlApt-137, or GL21.T-137 as indicated. After 24 h, cells were trypsinized, resuspended in medium serum free, and counted. Cells (1×10^5 in 100 μL serum-free medium per well) were then plated into the upper chamber of a 24-well transwell (Corning Incorporate, Corning, NY, USA) and exposed to 10% FBS as inducers of migration (0.6 mL, lower chamber). After 24 h, migrated cells were visualized by staining with 0.1% crystal violet in 25% methanol. The percentage of migrated cells was evaluated by eluting crystal violet with 1% SDS and reading the absorbance at 594-nm wavelength.

In Vivo Animal Study

A549 cells (5×10^6/mouse) were injected subcutaneously into flanks of 8-week-old NOD/SCID nude mice (Charles River). When tumor masses reached about 3 mm in length), mice were divided into three groups of three and intra-peritoneal injected with either PBS, GL21.T, or GL21.T-137 (1600 pmol in 100 μL/injection, three injections/week). After 1 week, tumor masses were measured by microcallipers and calculated according to the following formula: tumor volume (mm^3) = $L \times W^2/2$, where L is the length and W is the width. Animals were then scarified and tumors were excised and stored in 10% paraffin for histological examinations. Sections of 4–5 mm of tumors were deparaffinized and stained with H&E.

The animal experiments were approved by the Animal Ethics Committee of the Italian Ministry of Health.

Statistical Analysis

Statistics were analyzed with the Student's t test for comparisons between two groups or by ANOVA for multiple analyses.

SUPPLEMENTAL INFORMATION

Supplemental Information can be found online at https://doi.org/10.1016/j.omtn.2019.06.002.

AUTHOR CONTRIBUTIONS

S.N. and S.C. designed and performed the majority of the experiments, interpreted results, and assisted with manuscript preparation. M.C. performed and/or assisted with several experiments. A.F. provided human lung biopsies. P.S. provided useful reagents and advice. F.d.N. and S.B. performed and contributed to interpreting the *in vivo* experiments. C.L.E. coordinated the research, secured the funding, and guided the experimental design and the preparation of the manuscript.

CONFLICTS OF INTEREST

The authors declare no competing interests.

ACKNOWLEDGMENTS

We wish to thank V. de Franciscis for suggestions and L. Baraldi and F. Moscato for technical assistance. This work was supported by funds from the Italian Ministry of Health (GR-2011-02352546 to C.L.E.) and TERABIO.

REFERENCES

1. Tsao, A.S., Scagliotti, G.V., Bunn, P.A., Jr., Carbone, D.P., Warren, G.W., Bai, C., de Koning, H.J., Yousaf-Khan, A.U., McWilliams, A., Tsao, M.S., et al. (2016). Scientific Advances in Lung Cancer 2015. J. Thorac. Oncol. *11*, 613–638.

2. American Cancer Society (2017). Cancer Facts & Figures 2017 (American Cancer Society).

3. Economopoulou, P., and Mountzios, G. (2018). The emerging treatment landscape of advanced non-small cell lung cancer. Ann. Transl. Med. *6*, 138.

4. de Nigris, F. (2016). Epigenetic regulators: Polycomb-miRNA circuits in cancer. Biochim. Biophys. Acta *1859*, 697–704.

5. Hosseinahli, N., Aghapour, M., Duijf, P.H.G., and Baradaran, B. (2018). Treating cancer with microRNA replacement therapy: A literature review. J. Cell. Physiol. *233*, 5574–5588.

6. Lu, Z., Wang, M., Wu, S., Ye, M., Lin, Z., Shun, T., and Duan, C. (2018). MicroRNA-137-regulated AKT serine/threonine kinase 2 inhibits tumor growth and sensitizes cisplatin in patients with non-small cell lung cancer. Oncol. Lett. *16*, 1876–1884.

7. Chen, R., Zhang, Y., Zhang, C., Wu, H., and Yang, S. (2017). miR-137 inhibits the proliferation of human non-small cell lung cancer cells by targeting SRC3. Oncol. Lett. *13*, 3905–3911.

8. Zhu, X., Li, Y., Shen, H., Li, H., Long, L., Hui, L., and Xu, W. (2013). miR-137 inhibits the proliferation of lung cancer cells by targeting Cdc42 and Cdk6. FEBS Lett. *587*, 73–81.

9. Zhang, B., Liu, T., Wu, T., Wang, Z., Rao, Z., and Gao, J. (2015). microRNA-137 functions as a tumor suppressor in human non-small cell lung cancer by targeting SLC22A18. Int. J. Biol. Macromol. *74*, 111–118.

10. Catuogno, S., Esposito, C.L., Condorelli, G., and de Franciscis, V. (2018). Nucleic acids delivering nucleic acids. Adv. Drug Deliv. Rev. *134*, 79–93.

11. Catuogno, S., Esposito, C.L., and de Franciscis, V. (2016). Aptamer-mediated targeted delivery of therapeutics: an update. Pharmaceuticals (Basel) *9*, E69.

12. Dassie, J.P., Liu, X.Y., Thomas, G.S., Whitaker, R.M., Thiel, K.W., Stockdale, K.R., Meyerholz, D.K., McCaffrey, A.P., McNamara, J.O., 2nd, and Giangrande, P.H. (2009). Systemic administration of optimized aptamer-siRNA chimeras promotes regression of PSMA-expressing tumors. Nat. Biotechnol. *27*, 839–849.

13. Gilboa-Geffen, A., Hamar, P., Le, M.T., Wheeler, L.A., Trifonova, R., Petrocca, F., Wittrup, A., and Lieberman, J. (2015). Gene knockdown by EpCAM aptamer-siRNA chimeras suppresses epithelial breast cancers and their tumor-initiating cells. Mol. Cancer Ther. *14*, 2279–2291.

14. Wheeler, L.A., Vrbanac, V., Trifonova, R., Brehm, M.A., Gilboa-Geffen, A., Tanno, S., Greiner, D.L., Luster, A.D., Tager, A.M., and Lieberman, J. (2013). Durable knockdown and protection from HIV transmission in humanized mice treated with gel-formulated CD4 aptamer-siRNA chimeras. Mol. Ther. *21*, 1378–1389.

15. Zhou, J., Li, H., Zhang, J., Piotr, S., and Rossi, J. (2011). Development of cell-type specific anti-HIV gp120 aptamers for siRNA delivery. J. Vis. Exp. *52*, 2954.

16. Esposito, C.L., Cerchia, L., Catuogno, S., De Vita, G., Dassie, J.P., Santamaria, G., Swiderski, P., Condorelli, G., Giangrande, P.H., and de Franciscis, V. (2014). Multifunctional aptamer-miRNA conjugates for targeted cancer therapy. Mol. Ther. *22*, 1151–1163.

17. Catuogno, S., Rienzo, A., Di Vito, A., Esposito, C.L., and de Franciscis, V. (2015). Selective delivery of therapeutic single strand antimiRs by aptamer-based conjugates. J. Control. Release *210*, 147–159.

18. Esposito, C.L., Nuzzo, S., Kumar, S.A., Rienzo, A., Lawrence, C.L., Pallini, R., Shaw, L., Alder, J.E., Ricci-Vitiani, L., Catuogno, S., and de Franciscis, V. (2016). A combined microRNA-based targeted therapeutic approach to eradicate glioblastoma stem-like cells. J. Control. Release *238*, 43–57.

19. Russo, V., Paciocco, A., Affinito, A., Roscigno, G., Fiore, D., Palma, F., Galasso, M., Volinia, S., Fiorelli, A., Esposito, C.L., et al. (2018). Aptamer-miR-34c Conjugate Affects Cell Proliferation of Non-Small-Cell Lung Cancer Cells. Mol. Ther. Nucleic Acids *13*, 334–346.

20. Amarzguioui, M., and Rossi, J.J. (2008). Principles of Dicer substrate (D-siRNA) design and function. Methods Mol. Biol. *442*, 3–10.

21. Cerchia, L., Esposito, C.L., Camorani, S., Rienzo, A., Stasio, L., Insabato, L., Affuso, A., and de Franciscis, V. (2012). Targeting Axl with an high-affinity inhibitory aptamer. Mol. Ther. *20*, 2291–2303.

22. Thiel, W.H., Thiel, K.W., Flenker, K.S., Bair, T., Dupuy, A.J., McNamara, J.O., 2nd, Miller, F.J., and Giangrande, P.H. (2015). Cell-internalization SELEX: method for identifying cell-internalizing RNA aptamers for delivering siRNAs to target cells. Methods Mol. Biol. *1218*, 187–199.

23. Dassie, J.P., and Giangrande, P.H. (2013). Current progress on aptamer-targeted oligonucleotide therapeutics. Ther. Deliv. *4*, 1527–1546.

24. Wimmel, A., Glitz, D., Kraus, A., Roeder, J., and Schuermann, M. (2001). Axl receptor tyrosine kinase expression in human lung cancer cell lines correlates with cellular adhesion. Eur. J. Cancer *37*, 2264–2274.

25. Shieh, Y.S., Lai, C.Y., Kao, Y.R., Shiah, S.G., Chu, Y.W., Lee, H.S., and Wu, C.W. (2005). Expression of axl in lung adenocarcinoma and correlation with tumor progression. Neoplasia *7*, 1058–1064.

26. Ishikawa, M., Sonobe, M., Nakayama, E., Kobayashi, M., Kikuchi, R., Kitamura, J., Imamura, N., and Date, H. (2013). Higher expression of receptor tyrosine kinase Axl, and differential expression of its ligand, Gas6, predict poor survival in lung adenocarcinoma patients. Ann. Surg. Oncol. *20* (*Suppl 3*), S467–S476.

27. Qu, X., Liu, J., Zhong, X., Li, X., and Zhang, Q. (2016). Role of AXL expression in non-small cell lung cancer. Oncol. Lett. *12*, 5085–5091.

28. Iida, K., Sakai, R., Yokoyama, S., Kobayashi, N., Togo, S., Yoshikawa, H.Y., Rawangkan, A., Namiki, K., and Suganuma, M. (2017). Cell softening in malignant progression of human lung cancer cells by activation of receptor tyrosine kinase AXL. Sci. Rep. *7*, 17770.

29. Wu, F., Li, J., Jang, C., Wang, J., and Xiong, J. (2014). The role of Axl in drug resistance and epithelial-to-mesenchymal transition of non-small cell lung carcinoma. Int. J. Clin. Exp. Pathol. *7*, 6653–6661.

30. Tian, Y., Zhang, Z., Miao, L., Yang, Z., Yang, J., Wang, Y., Qian, D., Cai, H., and Wang, Y. (2016). Anexelekto (AXL) Increases Resistance to EGFR-TKI and Activation of AKT and ERK1/2 in Non-Small Cell Lung Cancer Cells. Oncol. Res. *24*, 295–303.

31. Iaboni, M., Fontanella, R., Rienzo, A., Capuozzo, M., Nuzzo, S., Santamaria, G., Catuogno, S., Condorelli, G., de Franciscis, V., and Esposito, C.L. (2016). Targeting Insulin Receptor with a Novel Internalizing Aptamer. Mol. Ther. Nucleic Acids *5*, e365.